All-Printed Paper Memory

Der-Hsien Lien,[†,‡] Zhen-Kai Kao,[§] Teng-Han Huang,[†] Ying-Chih Liao,[§,*] Si-Chen Lee,[‡,∥,*] and Jr-Hau He[†,∥,⊥,*]

[†]Institute of Photonics and Optoelectronics, [‡]Institute of Electronics Engineering, [§]Department of Chemical Engineering, and [∥]Department of Electrical Engineering, National Taiwan University, Taipei 10617, Taiwan, and [⊥]Computer, Electrical and Mathematical Sciences and Engineering (CEMSE) Division, King Abdullah University of Science & Technology (KAUST), Thuwal 23955-6900, Saudi Arabia

ABSTRACT We report the memory device on paper by means of an all-printing approach. Using a sequence of inkjet and screen-printing techniques, a simple metal—insulator—metal device structure is fabricated on paper as a resistive random access memory with a potential to reach gigabyte capacities on an A4 paper. The printed-paper-based memory devices (PPMDs) exhibit reproducible switching endurance, reliable retention, tunable memory window, and the capability to operate under extreme bending conditions. In addition, the PBMD can be labeled on electronics or living objects for multifunctional, wearable, on-skin, and biocompatible applications. The disposability and the high-security data storage of the paper-based memory are also demonstrated to show the ease of data handling, which are not achievable for regular silicon-based electronic devices. We envision that the PPMDs manufactured by this cost-effective and time-efficient all-printing approach would be a key electronic component to fully activate a paper-based circuit and can be directly implemented in medical biosensors, multifunctional devices, and self-powered systems.

KEYWORDS: paper electronics · inkjet printing · resistive random access memory · flexible electronics

Paper, a revolutionary lightweight writing medium invented by Lun Cai in 105, began its impact on human writing systems as a replacement for pieces of silk (costly) and tablets of bamboo (heavy).[1] Later, the printing system using movable type, first created by Sheng Bi in 1040 and then improved by Johannes Gutenberg in 1439, revolutionized communication and book production.[2,3] From then on the data storage capability of paper has tremendously increased, leading to a rapid spread of knowledge and thriving of world civilization. In the 1960s, the invention of marks and punched tapes/cards allowed machines to quickly write/read data on paper. However, paper was still a WORM (Write Once, Read Many) device. Due to the rapid development of modern microelectronics in the past few decades, the role of the paper as the main data container/messenger is being replaced by a variety of electronic devices that are often implemented on rigid substrates (*e.g.*, optical discs, hard disk drives (magnetic), and flash memory (capacitance)).

Recently, with more interest in cheap, simple, and energy-saving fabrication processes for microelectronics, much attention has been focused on making electronic devices using printing techniques on any desired substrates, especially so-called flexible electronics.[4,5] Printed and flexible electronics is expected to reach $45 billion by 2016, and paper-based electronics shows great potential to meet this increasing demand due to its popularity, flexibility, foldability, low cost, mass productivity, disposability, retrievability, nonpollution, and ease of processing.[4,6] Up to now, diverse types of electronic components on paper substrates have been invented, including conducting wires, resistors, capacitors, transistors, and diodes.[7−13] Integrating multiple components into a functional circuit subsequently has led to fantastic applications, such as 3D antennas,[10] radio frequency identification (RFID) tags,[14] and cellulose-based batteries.[9] However, to fully activate a paper-based circuit, the memory device, a key component in charge of programing, data storage, and system setting, is still needed.

The challenge of manufacturing memory devices on paper arises from the difficulties of device fabrication on paper. Typically, memory devices require thin and uniform layers, but paper substrates are rough and porous due to their fibrous nature. Moreover, although volatile memories have been demonstrated on paper substrates,

* Address correspondence to jhhe@cc.ee.ntu.edu.tw; sclee@cc.ee.ntu.edu.tw; liaoy@ntu.edu.tw.

Received for review March 3, 2014 and accepted July 14, 2014.

Published online July 14, 2014
10.1021/nn501231z

an embedded power source can severely degrade the portability and is unrealistic in paper-based electronic systems.[15] Regarding these concerns, a simple-geometry electronic memory on paper, regardless of a consecutive power supply, is particularly desirable. Resistive random access memory (RRAM), an emerging type of nonvolatile memory, is the most suitable solution for paper-related applications. Such memory is operated by changing the resistances of a formulated insulator material, whose resistive states ("0" and "1") vary greatly as different voltages are imposed across it.[16] Structural simplicity is a major advantage of RRAM: only one insulator and two electrodes are required for a bit.

The realization of paper memory relies on a fabrication technique compatible with the paper substrates. Conventional techniques, such as chemical vapor deposition and sputtering techniques, usually require vacuum and high-temperature conditions. Considering the fabrication environment and chemical compatibility, most of these fabrication processes are not suitable for paper-based device fabrication. Alternatively, printing technologies, such as screen printing, inkjet printing, microcontact printing, and 3D printing, are more efficient and flexible fabrication processes[17] and are appropriate for paper-based electronics with versatile applications, such as batteries, wearable antennas, supercapacitors, nanogenerators, and displays.[18−22] In addition, paper-based devices can realize low-cost electronics (<2 cents), compared with conventional components (~5 cents per piece).[6] Recently, a printed RRAM has been fabricated on flexible substrates and has shown great performance.[23,24] Similar nanostructured insulator/metal layers might also be applied on paper substrates to form RAAM devices with appropriate printing techniques.[25]

In this study, we implemented the emerging nonvolatile memory electronics into a conventional data storage medium, "paper", to demonstrate the first all-printed electronic paper memory with a simple metal−insulator−conductor structure (silver/TiO_2/carbon, Ag/TiO_2/C). The printed-paper-based memory device (PPMD) exhibits high reliability in terms of cycling endurance and data retention, with a tunable ON/OFF memory window (up to 3 orders of magnitude) *via* tuning the thickness of the TiO_2 layer. The PPMD also shows excellent device performance even under extreme bending conditions, indicating its mechanical robustness. As fabricated on an adhesive label, PPMD is also capable of being intimately, tightly, and reliably affixed to the surface of any material, including electronic devices and living subjects, with high-performance nonvolatile functionality. This feature facilitates the use of memory devices as a component in a flexible, wearable, and biocompatible electronic system. Compared with the complex, time-consuming, secure data destruction for conventional memory devices on rigid or polymer substrates, such as degaussing or software-based erasing/overwriting, permanent removal of secure data from the PPMD can be achieved simply by burning or shredding. Finally, as the fabrication of paper memory is based on all-printing processes, the estimated price is only ~0.0003 cent/bit. We envision that the PPMD can facilitate the development of paper-based circuits, which can be implemented in medical biosensors and self-powered and multifunctional devices.

RESULTS AND DISCUSSION

Figure 1a illustrates the fabrication process and the device layout of the printed paper memory (see Methods and Supporting Information). In short, the paper substrate was coated with carbon (C) paste as the bottom electrode *via* screen printing. Then, an active layer of TiO_2 nanoparticles was inkjet printed on the C bottom electrodes. After the TiO_2 layer was dried, dots of silver (Ag) nanoparticle ink were printed on the TiO_2 layer as the top electrodes. The as-printed Ag electrode was cured to show conductivity after a sintering process at 180 °C for 1 h (see Supporting Information for details).[26] The employment of inkjet printing features three unique advantages: (i) the patterns of the memories are digitally controllable with a high degree of freedom without using any lithography technique. For example, as shown in Figure 1b and c, the memory cells can be printed as alphabetical letters ("NTU": abbreviation for National Taiwan University) or dot arrays (with 18 cells in a row). The width of the TiO_2 layer is ~700 μm, and the diameter of the Ag electrode is ~300 μm. (ii) Each layer of the memory can be deposited

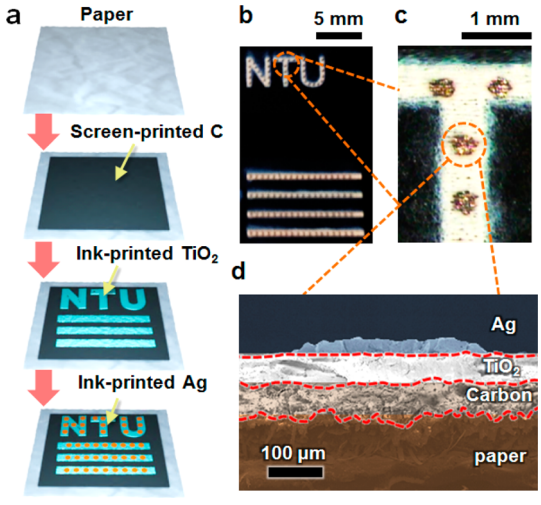

Figure 1. Fabrication and geometry of a paper RRAM. (a) Schematic diagram of the fabrication process for the resistive paper memory device. (b) Photograph of the device taken by optical microscopy. The alphabetical letters and the line arrays composed of Ag and TiO_2 demonstrate the degree of freedom for the inkjet-printed patterns. (c) Zoom-in optical image from b. (d) Cross-sectional scanning electron microscopy image of the paper-based memory.

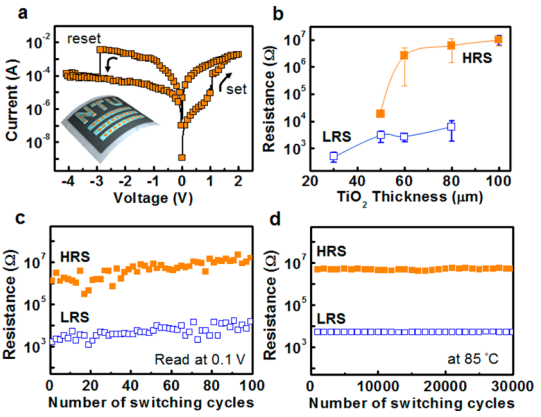

Figure 2. Characteristics of the paper memory. (a) *I*−*V* characteristics of a paper memory. The inset is an optical microscopy image of the device and an illustration of the probe measurement setup, where the voltage bias is applied on the Ag electrode and the C electrode is grounded. (b) Memory window as a function of printed TiO_2 layer thickness. (c) Endurance cycles of the paper memory devices. The reading voltage is 0.1 V. (d) Retention times of the paper memory devices characterized at 85 °C.

on paper substrates with high uniformity. Excellent structural uniformity was further confirmed by scanning electron microscopy, as shown in Figure 1d. No agglomerations were observed, indicating the excellent dispersion of each printed layer. Because the roughness issue is crucial in fabricating printed electronic components on paper (for printing papers ~10 μm), additional coating or polishing processes are usually required to achieve a smoother and less nonabsorptive surface, while these features compromise the low cost and recyclability.[6] The advantage of our approach is that by the sequential printing processes the roughness is gradually smoothed by depositing upper layers (Figure 1d), which is difficult for any single printing process. Additionally, like normal inkjet printing, each printed layer is tightly embedded onto the paper, and therefore the devices retain flexibility. (iii) The current work used a regular inkjet printing method that has a dot size of ~50 μm with a pitch resolution of 25 μm. Thus, one bit will occupy a square of ~100 μm on each side, or 10^4 bit/cm^2. With that density, a fully printed A4 paper can have ~1 MB. With a better printer (superfine inkjet, SIJ Technology), one can achieve a dot resolution of <1 μm and nearly the same pitch width. Therefore, the density can be enhanced by ~2500 times, and >1 GB can be obtained on one A4 paper.

With the sound device structure configuration, the PPMD showed well-defined memory-switching behaviors. Figure 2a presents typical current−voltage (*I*−*V*) switching characteristics of a paper-based resistive memory device. Pristine devices are in high resistance states (HRS, OFF state) and can be directly operated without an electroforming process, which is significantly beneficial from the viewpoint of RRAM circuit operation. Without electroforming, the memory devices on papers show uniform performance and reproducible switching operation by both dc voltage sweeping and ac voltage pulses. By applying a positive set voltage exceeding 1 V, the current abruptly increases, followed by a resistive switch from HRS to low resistance state (LRS, ON state). The ON state can be retained after the applied bias is off, showing a nonvolatile memory behavior.[27] To turn OFF the device, a negative bias is applied (reset voltage ≈ −3 V), inducing a sudden decrease of current and turning the memory into an HRS. This switching type achieved by sequentially applying voltages with opposite polarity is bipolar switching.[24,28] The switching mechanism can be explained by the electrochemical metalization, relying on the electrochemical dissolution of a mobile metal (*e.g.*, Ag) to perform the ON/OFF switching operation.[29] Note that the states of the printed TiO_2 layer itself cannot be switched without the deposition of inkjet-printed Ag electrodes, which demonstrates the role of Ag as the source for conducting nanofilaments, in agreement with previous reports.[27] Moreover, we noted that previous C-based materials have been demonstrated to be stable electrodes and switching materials.[30,31] In this work, the Ag/TiO_2/C structure can be referred to as conductive-nanobridge RRAM, recognized as the formation and the rupture of the Ag conductive nanobridge within the dielectric TiO_2 electrolyte.[32] As such, a porous structure featuring a high permeability for metal atoms/ions is preferable. Since the TiO_2 ink is made of nanoparticles, the structure is naturally porous and thus provides more chances to form conductive nanobridges. This feature results in a forming-free characteristic of our memory with a device yield of over 90%, which represents a significant simplification for practical uses.

Another important advanced feature of the PPMDs is their tunable memory window achieved by a modulation of the insulator thickness *via* controlling inkjet printing times of TiO_2 nanoparticles. Figure 2b shows a statistical analysis of HRS and LRS with relation to the inkjet-printing TiO_2 thickness. It shows that a thin TiO_2 layer (thickness <40 μm) keeps the device in an LRS due to Ag electrodes directly penetrating through TiO_2 to the C electrodes and leads to no memory window. When the TiO_2 layer is thick enough (thickness >50 μm), the memory window appears and gradually enlarges with TiO_2 layer thickness possibly because of the increase in serial resistance of the TiO_2 layer.[33] When the TiO_2 layer thickness is more than 100 μm, the devices become pure insulators and cannot be operated. Overall, the ON/OFF ratio ranges from 10 to 10^3. More details about the RRAM characterization can be found in the Supporting Information. Taking advantage of the inkjet printing technique, the tunable window provides a broad range of reading margins according to the requirement and the sensitivity of the external management systems.[34] Note that a thickness of 80 μm allows the device to perform with the highest ON/OFF ratio and is used hereinafter.

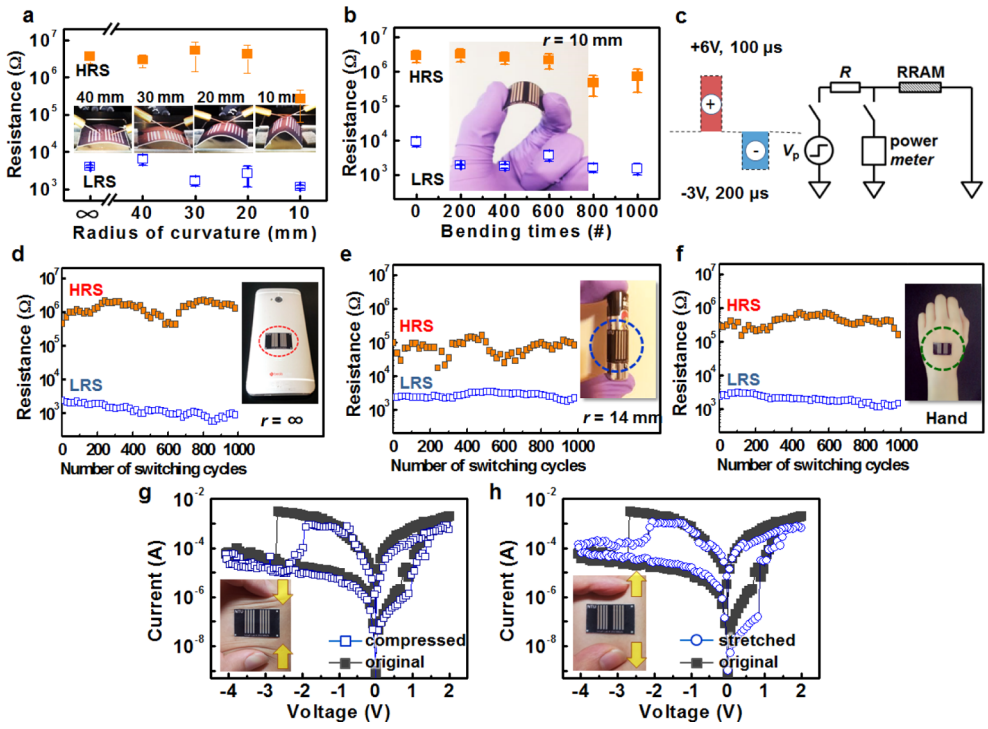

Figure 3. Bending test and on-chip and on-skin applications. (a) ON/OFF distribution as a function of bending radius of curvature. The inset shows a series of optical images under different bent conditions. (b) ON/OFF distribution as a function of bending time with a bending radius of ~10 mm. (c) Illustration of the equivalent circuit for the pulse measurement system. The inset illustrates the condition of input pulse, which is composed of a 100 μs and 6 V pulse as the write and a 200 μs and −3 V pulse as the erase. The reading voltage is 0.5 V. The switching characteristics of memory labels tagged on (d) a smart cellphone (flat surface: $r = \infty$), (e) an AA battery (r = 14 mm), and (f) undeformed skin of the human body. The switching characteristics of the paper memory on (g) compressed and (h) stretched skin of the human body.

An endurance test was carried out to further examine the multitime programmable capability of the PPMD. As shown in Figure 2c, the memory device was successively switched 100 times; meanwhile, the resistance values of the HRS and LRS were read at 0.1 V of dc. During 100 endurance cycles, both the HRS and the LRS retained their values without significant change under the reading bias, showing the reproducible switching capability of resistive paper memory. The retention property of the paper memory was also characterized at 85 °C, as shown in Figure 2d.[28] The resistance ratio of the resistive states was retained up to 3×10^4 s at 85 °C without electrical degradation, showing that the PPMD is capable of retaining data integrity at high temperatures. As a matter of fact, the data in PPMDs can be stored safely at temperatures up to 150 °C, as shown later in the thermal test section. Briefly, this is, to the best of our knowledge, the first nonvolatile electronic paper memory distinct from conventional simple mechanical paper tapes or punch cards.[6]

The flexibility of the device, responsible for foldable and wearable applications, is of practical importance. As shown in Figure 3a, the bending test was performed to verify if the PPMD can be reliably operated under bent conditions. The degree of bending is expressed by the radius of curvature (r) between two edges of the substrate, as drawn in the inset of Figure 3a and explained in the Supporting Information. The devices were operated by dc voltages with the conditions as described earlier. The statistical analysis including cycle-to-cycle and device-to-device tests for five cells provides convincing evidence for evaluating the resistive switching behaviors. For $r > 20$ mm, the same switching characteristics as that in the flat condition are observed. For $r = 10$ mm, the switch window decreases by 20% relative to the flat control. Notably, the memory window is reversible as the device returns from $r = 10$ mm to the flat condition. To highlight the mechanical robustness, the memory performances were monitored after repetitive bending for more than 1000 times with a bending radius of ~10 mm, as depicted in Figure 3b. The excellent device stability after successive bending with $r = 10$ mm confirms the excellent reliability of the flexible paper memory devices.

Another important feature of the paper memory is that it can be used as a label on the surface of any article (including electronic and storage devices) or living subject and still retain its code functions. The paper memory was fabricated on an adhesive label with identical processes as described above and then readily affixed to different objects. The paper memory devices were tested and triggered by ac pulses after adhesion. The equivalent circuit is plotted in Figure 3c.

The writing bias is the positive pulse with a height of 6 V and width of 100 μs, and the erasing bias is the negative pulse with a height of 3 V and width of 200 μs. The reading voltage is 0.5 V. Note that here a resistance of 500 Ω was applied in the circuit to restrain the current (compliance current) flowing through the devices. Figure 3d and e show the switching endurance of the PPMD tagged on different solid surfaces: a smart phone (flat surface: $r = \infty$) and an AA battery (r = 14 mm). As the input voltage pulses were applied in sequence 1000 times, the resistive values responding to ON and OFF states were recorded. The ON/OFF ratio for the flat surface (*i.e.*, a smart phone in Figure 3d) is slightly larger than the curved one (*i.e.*, an AA battery in Figure 3e), in accordance with the results in Figure 3a. The result indicates that the PPMD can be readily implemented into planar or nonplanar electronic devices with stable switching properties. As shown in Figure 3f–h, we further demonstrated the use of paper memories as on-skin stickers conforming to living subjects, *e.g.*, human bodies. Note that as the paper is made of cellulose, it is biocompatible and suitable for wearable applications.[35] The memory can be successfully affixed to the back of the hand, as demonstrated in the inset of Figure 3f, and does not irritate the skin after long-term use. The paper memory device stuck to undeformed skin also triggered by electrical pulses shows stable switching behaviors during 1000 replications (Figure 3f). As shown in Figure 3g,h, the paper memory devices on compressed and stretched skin are still switchable and operate normally, respectively. These tests demonstrate that the printed paper memory stickers with excellent switching characteristics supple enough to conform to a variety of objects could enable the use of memory devices as a component in a flexible, wearable, and biocompatible electronic system for the first time.

To secure sensitive data from disclosure or being stolen, data removal is an important issue, particularly in military or commercial uses. Typically, data elimination is carried out by complex, time-consuming physical destruction, insecure degaussing, or software-based erasing/overwriting. Owing to mechanical robustness of semiconductor memories and advanced recovery technique, permanent data elimination is hard to manipulate. A major advantage of the paper-based memory demonstrated here is its disposability. Here two examples are shown to demonstrate the ease of data removal of the paper-based memories for security purposes. First, the data can be totally and irreversibly eliminated by burning, simply by lighting a match or heating over 250 °C. The temperature-dependent switching performance is shown in Figure 4a. Below 150 °C, the memory devices can retain the ON/OFF ratio without significant electrical degradation, demonstrating their stability under extreme weather conditions. Note that paper substrates do not deform

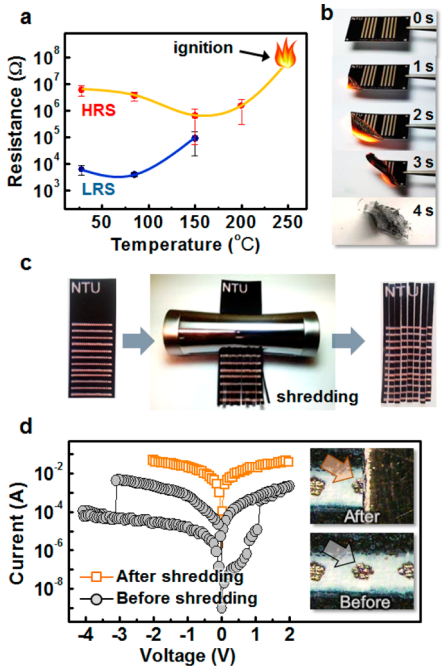

Figure 4. Thermal test and security demonstration. (a) Variation of resistive switching states as a function of environmental temperature. (b) Sequence of pictures showing the ignition process of the paper memory at 250 °C within 4 s, leading to permanent data removal. (c) Image of paper memory before and after being shredded by a shredder. (d) *I*–*V* characteristics of a paper memory before and after being shredded, and the corresponding optical microscopy images.

as much as low-cost plastics do upon heating, which is an important issue for harsh-environment applications.[36–38] At temperatures higher than 150 °C, the memory window gradually shrunk and the difference between the two states became indistinguishable since the resistance of the HRS and LRS was decreased and increased with temperature, respectively. Then, a higher temperature (>250 °C) caused the paper fibers to darken and the cellulose decomposed within 5s, leading to a permanent failure of the device (Figure 4b). Paper shredding is another efficient way to securely remove the data from the paper-based memory, as shown in Figure 4c. For traditional paper documents, shredders supposedly destroy the paper document. However, it can be reconstructed by piecing together the series of shredded documents *via* recognizing the text on the documents. On the other hand, when the paper memory is shredded, each piece looks identically the same (Figure 4c) and thus is hard to identify and recover. Figure 4d is an example showing the *I*–*V* characteristics of a paper memory before and after shredding. We first selected a memory device and operated it several times to ensure its operation status before shredding. Then, the device was shredded by a shredder and measured again. The paper memory device failed to switch and showed pure resistance (~58 Ω) after shredding, which is even lower than the LRS of paper memory (before shredding), indicating a

leakage through the TiO_2 nanoparticle layer. This result shows that direct paper memory shredding can lead to permanent data elimination. In brief, these two examples are demonstrated here to show the emergent destruction of the paper memory device, inhibiting the recovery of classified information to the maximum extent possible within the time constraints.

The use of paper-based electronics rather than their commercial counterparts in existing products is also motivated by rapid manufacturing and cost effectiveness. For instance, paper is produced at a speed exceeding 10^6 m^2/h and has a cost of \$0.06 cent/$inch^2$, which is ~5 orders faster and 3−4 orders cheaper than those of monocrystalline Si wafers, which are the most commonly used substrates in the electronic industry (see Supporting Information). Combining the utilization of the paper substrates with printing techniques without using additional lithography techniques allows a time- and cost-effective scheme for the paper memory. Moreover, it is worth mentioning that the paper memory device demonstrated here has an estimated cost of ~0.0003 cent/bit (see Supporting Information). As for other printed devices, a fully printed RFID tag (1 bit) fabricated on a PET substrate is estimated to be 3 cent/bit,[14] credit-card-sized ID tags (96 bits) on paper have a cost less than 0.021 cent/bit,[39] and a sensor or authentication system on paper substrates costs ~0.1 to 1 cent.[40] The higher expense could be due to the complex structure, multiple fabrication processes, and larger areas per device. The time- and cost-effective scheme of an all-printed paper memory employed in this study provides an ideal option to be integrated in existing devices.

CONCLUSIONS

In conclusion, for the first time we fabricated a nonvolatile memory on paper using an all-printing approach. The paper-based memory shows excellent rewritable switching properties and capability to retain information. The paper memory exhibits stable endurance under extreme bending conditions, demonstrating promising characteristics of flexible electronics. A memory label was fabricated and affixed to other electronic devices and biological objects, showing its excellent integrative and biocompatible characteristics. Finally, we demonstrated the disposability and the capability of secure data removal of the paper memory, which is not achievable for other electronic devices integrated on rigid substrates. The idea for developing penny-cost all-printed paper memory (as low as ~0.0003 cent/bit) demonstrated here will expand flexible, printed electronics into a new line of applications in security printing, identification, advertising, warning, and epidermal electronics.[41]

METHODS

Fabrication Process. Carbon paste (Acheson-Henkel, Taiwan) was first coated on commercial printing paper by a screen printer (RJ-55AC, Houn Jien Co., Ltd.). The process was repeated 10 times to reduce the surface roughness of the paper, and then the samples were cured for 10 min at 100 °C in a vacuum oven. The screen mold is made of polyester with the following conditions: mesh count, 150 mesh/inch; mesh opening, 100 μm; thread diameter, 50 μm; open surface, 35%; fabric thickness, 80 μm. The second step was to deposit the TiO_2 layer on the paper with carbon bottom electrodes. The preparation of the TiO_2 ink is as follows: 0.5 g of TiO_2 nanoparticles ~25 nm in diameter (Sigma Inc.) was mixed into a solvent of 50 μL of acetyl acetone (Alfa Aesar), 50 μL of Triton-X-100 (Acros), 8.5 mL of DI water, 1 mL of ethanol, and 0.5 mL of ethylene glycol. The inkjet printing was done by a MicroFab JetLab4 system (MicroFab Technologies Inc.) with two piezoelectric nozzles, 50 μm in diameter. TiO_2 ink was deposited at a temperature of 50 °C. After the TiO_2 layers dried, the Ag layer was printed on the TiO_2 layer as the top electrodes. The Ag ink was prepared by adding 10 wt % Ag nanoparticles into a humectant solution (30% ethylene glycol and 70% water). The Ag nanoparticles have a mean diameter of 200 nm (see Supporting Information for details). To disperse the nanoparticles better, the as-made ink was put in a sonication bath for 2 h. The size and the velocity of the ejected droplets were measured through an optical image analysis system. For both TiO_2 and Ag inks, the diameters of the ejected droplets were ~50 μm. The drop ejection frequency was controlled at 1000 Hz, with ejection velocities of 1.86 m/s for TiO_2 ink and 2.6 m/s for Ag ink.

Memory Characteristics. Morphological studies have been performed with a JEOL JSM-6500 field-emission scanning electron microscope. The electrical characteristics were carried out using a Keithley 4200 semiconductor parameter analyzer. The bending test was conducted by mounting the devices on homemade stages with confined gaps. The electrical pulse was trigged by a function generator (33250A, Agilent Technology), and a resistance of 500 Ω was used to confine the current flowing through the device. When conducting the pulse switching, the resistance of the memory was measured by a power-meter (B2902A, Agilent Technology). All of the operation voltages were applied on the Ag top electrode, and the carbon bottom electrode was grounded. During the measurement in the voltage sweeping mode, the positive bias is defined as the current flow from the top to the bottom electrodes, and the negative bias was defined as the direction from the bottom to the top electrodes.

Conflict of Interest: The authors declare no competing financial interest.

Supporting Information Available: Preparation of the TiO_2 ink, sintering parameters of the Ag ink, electrical characteristics of the inkjet-printed Ag, switching parameters as a function of TiO_2 thickness, bending test of the flexible all-printed paper memory, fabrication speed of paper and Si wafer, and cost of the paper memory. This material is available free of charge *via* the Internet at http://pubs.acs.org.

Acknowledgment. We thank W.W.C., P.K.Y., S.H.D., and H.C.F. for technical support and helpful discussions. This work was supported by the National Science Council of Taiwan (99-2622-E-002-019-CC3, 99-2112-M-002-024-MY3, 99-2120-M-007-011, and 101-2221-E-002-177-MY2).

REFERENCES AND NOTES

1. Fan, Y. *The Book of the Later Han Dynasty*, Vol. 78, p 445.
2. Shen, K. *Dream Pool Essays*, Vol. 18, p 1088.
3. Kapr, A. *Johann Gutenberg: The Man and His Invention*; Scholar Press: Aldershot, 1985.
4. Wang, C.; Hwang, D.; Yu, Z.; Takei, K.; Park, J.; Chen, T.; Ma, B.; Javey, A. User-Interactive Electronic Skin for

Instantaneous Pressure Visualization. *Nat. Mater.* **2013**, *12*, 899–904.
5. Wang, X.; Liu, B.; Wang, Q.; Song, W.; Hou, X.; Chen, D.; Cheng, Y. b.; Shen, G. Three-Dimensional Hierarchical $GeSe_2$ Nanostructures for High Performance Flexible All-Solid-State Supercapacitors. *Adv. Mater.* **2013**, *25*, 1479–486.
6. Tobjork, D.; Osterbacka, R. Paper Electronics. *Adv. Mater.* **2011**, *23*, 1935–1961.
7. Harting, M.; Zhang, J.; Gamota, D. R.; Britton, D. T. Fully Printed Silicon Field Effect Transistors. *Appl. Phys. Lett.* **2009**, *94*, 193509.
8. Martins, R.; Ferreira, I.; Fortunato, E. Electronics with and on Paper. *Phys. Status Solidi: Rapid Res. Lett.* **2011**, *5*, 332–335.
9. Nystrom, G.; Razaq, A.; Stromme, M.; Nyholm, L.; Mihranyan, A. Ultrafast All-Polymer Paper-Based Batteries. *Nano Lett.* **2009**, *9*, 3635–3639.
10. Russo, A.; Ahn, B.; Adams, J.; Duoss, E.; Bernhard, J.; Lewis, J. Pen-on-Paper Flexible Electronics. *Adv. Mater.* **2011**, *23*, 3426–2430.
11. Siegel, A. C.; Phillips, S. T.; Dickey, M. D.; Lu, N.; Suo, Z.; Whitesides, G. M. Foldable Printed Circuit Boards on Paper Substrates. *Adv. Funct. Mater.* **2010**, *20*, 28–35.
12. Yang, L.; Cheng, S.; Ding, Y.; Zhu, X. B.; Wang, Z. L.; Liu, M. L. Hierarchical Network Architectures of Carbon Fiber Paper Supported Cobalt Oxide Nanonet for High-Capacity Pseudocapacitors. *Nano Lett.* **2012**, *12*, 321–325.
13. Yuan, L. G.; Xiao, X.; Ding, T. P.; Zhong, J. W.; Zhang, X. H.; Shen, Y.; Hu, B.; Huang, Y. H.; Zhou, J.; Wang, Z. W. Paper-Based Supercapacitors for Self-Powered Nanosystems. *Angew. Chem., Int. Ed.* **2012**, *51*, 4934–4938.
14. Jung, M.; Kim, J.; Noh, J.; Lim, N.; Lim, C.; Lee, G.; Kim, J.; Kang, H.; Jung, K.; Leonard, A. D.; *et al*. All-Printed and Roll-to-Roll-Printable 13.56-MHz-Operated 1-bit RF Tag on Plastic Foils. *IEEE Trans. Electron Devices* **2010**, *57*, 571–580.
15. Martins, R.; Barquinha, P.; Pereira, L.; Correia, N.; Gonçalves, G.; Ferreira, I.; Fortunato, E. Write-Erase and Read Paper Memory Transistor. *Appl. Phys. Lett.* **2008**, *93*, 203501.
16. Huang, C. H.; Huang, J. S.; Lin, S. M.; Chang, W.-Y.; He, J. H.; Chueh, Y. L. ZnO_{1-x} Nanorod Arrays/ZnO Thin Film Bilayer Structure: From Homojunction Diode and High-Performance Memristor to Complementary 1D1R Application. *ACS Nano* **2012**, *6*, 8407–8414.
17. Ladd, C.; So, J. H.; Muth, J.; Dickey, M. D. 3D Printing of Free Standing Liquid Metal Microstructures. *Adv. Mater.* **2013**, *25*, 5081–5085.
18. Lakafosis, V.; Rida, A.; Vyas, R.; Li, Y.; Nikolaou, S.; Tentzeris, M. M. Progress towards the First Wireless Sensor Networks Consisting of Inkjet-Printed, Paper-Based RFID-Enabled Sensor Tags. *Proc. IEEE* **2010**, *98*, 1601–1609.
19. Andersson, P.; Nilsson, D.; Svensson, P. O.; Chen, M. X.; Malmstrom, A.; Remonen, T.; Kugler, T.; Berggren, M. Active Matrix Displays Based on All-Organic Electrochemical Smart Pixels Printed on Paper. *Adv. Mater.* **2002**, *14*, 1460–1464.
20. Hu, L.; Wu, H.; Mantia, F. L.; Yang, Y.; Cui, Y. Thin, Flexible Secondary Li-Ion Paper Batteries. *ACS Nano* **2010**, *4*, 5843–5848.
21. Zheng, G.; Hu, L.; Hui, W.; Xie, X.; Cui, Y. Paper Supercapacitors by a Solvent-Free Drawing Method. *Energy Environ. Sci.* **2011**, *4*, 3368–3373.
22. Zhong, Q.; Zhong, J.; Hu, B.; Hu, Q.; Zhou, J.; Wang, Z. L. Fiber-Based Generator for Wearable Electronics and Mobile Medication. *Energy Environ. Sci.* **2013**, *6*, 1779–1784.
23. Mohapatra, S. R.; Tsuruoka, T.; Hasegawa, T.; Terabe, K.; Aono1, M. Flexible Resistive Switching Memory using Inkjet Printing of a Solid Polymer Electrolyte. *AIP Adv.* **2012**, *2*, 022144.
24. Yang, P. K.; Chang, W. Y.; Teng, P. Y.; Jen, S. F.; Lin, S. J.; Chiu, P. W.; He, J. H. Fully Transparent Resistive Memory Employing Graphene Electrodes for Eliminating Undesired Surface Effects. *Proc. IEEE* **2013**, *101*, 1732–1739.
25. Chiang, Y. D.; Chang, W. Y.; Ho, C. Y.; Chen, C. Y.; Ho, C. H.; Lin, S. J.; Wu, T. B.; He, J. H. Single-ZnO-Nanowire Memory. *IEEE Trans. Electron Devices* **2011**, *58*, 1735–1740.
26. Kao, Z. K.; Hung, Y. H.; Liao, Y. C. Formation of Conductive Silver Films *via* Inkjet Reaction System. *J. Mater. Chem.* **2011**, *21*, 18799–18803.
27. Tsunoda, K.; Fukuzumi, Y.; Jameson, J. R.; Wang, Z.; Griffin, P. B.; Nishi, Y. Bipolar Resistive Switching in Polycrystalline TiO_2 Films. *Appl. Phys. Lett.* **2007**, *90*, 113501.
28. Lee, M. J.; Lee, C. B.; Lee, D.; Lee, S. R.; Chang, M.; Hur, J. H.; Kim, Y. B.; Kim, C. J.; Seo, D. H.; Seo, S.; *et al*. A Fast, High-endurance and Scalable Non-volatile Memory Device Made from Asymmetric Ta_2O_{5-x}/TaO_{2-x} Bilayer Structures. *Nat. Mater.* **2011**, *10*, 625–630.
29. Mikolajick, T.; Salinga, M.; Kund, M.; Kever, T. Nonvolatile Memory Concepts Based on Resistive Switching in Inorganic Materials. *Adv. Eng. Mater.* **2009**, *11*, 235–240.
30. Chai, Y.; Wu, Y.; Takei, K.; Chen, H.-Y.; Yu, S.; Chan, P. C. H.; Javey, A.; Wong, H. S. P. *Resistive Switching of Carbon-Based RRAM with CNT Electrodes for Ultra-dense Memory*; IEEE, IEDM Technical Digest: San Francisco, CA, 2010; pp 214−217.
31. Chai, Y.; Wu, Y.; Takei, K.; Chen, H.-Y.; Yu, S.; Chan, P. C. H.; Javey, A.; Wong, H. S. P. Nanoscale Bipolar and Complementary Resistive Switching Memory Based on Amorphous Carbon. *IEEE Trans. Electron Devices* **2011**, *58*, 3933–3939.
32. Waser, R.; Aono, M. Nanoionics-Based Resistive Switching Memories. *Nat. Mater.* **2007**, *2*, 833–840.
33. Tedesco, J. L.; Stephey, L.; Hernandez, M. M.; Ritcher, C. A.; Gergel, H. N. Switching Mechanisms in Flexible Solution-Processed TiO_2 Memristors. *Nanotechnology* **2012**, *23*, 305206.
34. Brown, W. D.; Brewer, J. *Nonvolatile Semiconductor Memory Technology; A Comprehensive Guide to Understanding and Using NVSM Devices*; Wiley-IEEE Press: New York City, 1998.
35. Lee, C. H.; Hankus, M. E.; Tian, L.; Pellegrino, P. M.; Singamaneni, S. Highly Sensitive Surface Enhanced Raman Scattering Substrates Based on Filter Paper Loaded with Plasmonic Nanostructures. *Anal. Chem.* **2011**, *83*, 8953–8958.
36. Huang, T. H.; Chang, W. Y.; Chien, J. F.; Kang, C. F.; Yang, P. K.; Chen, M. J.; He, J. H. Eliminating Surface Effects *via* Eemploying Nitrogen Doping to Significantly Improve the Stability and Reliability of ZnO Resistive Memory. *J. Mater. Chem. C* **2013**, *1*, 7593–7597.
37. Huang, T. H.; Yang, P. K.; Lien, D. H.; Kang, C. F.; Tsai, M. L.; Chueh, Y. L.; He, J. H. Metal Oxide Resistive Memory for Harsh Electronics: Immunity to Surface Effect and High Corrosion Resistance *via* Surface Modification. *Sci. Rep.* **2014**, *4*, 4402.
38. Ke, J. J.; Liu, Z. J.; Kang, C. F.; Lin, S. J.; He, J. H. Surface Effect on Resistive Switching Behaviors of ZnO. *Appl. Phys. Lett.* **2011**, *99*, 192106.
39. Weigelt, K.; Hambsch, M.; Karacs, G.; Zillger, T.; Hubler, A. C. Labeling the World: Tagging Mass Products with Printing Processes. *IEEE Pervasive Comput.* **2010**, *9*, 59–63.
40. Berggren, M.; Nilsson, D.; Robinson, N. D. Organic Materials for Printed Electronics. *Nat. Mater.* **2007**, *6*, 3–5.
41. Kim, D. H.; Lu, N. S.; Ma, R.; Kim, Y. S.; Kim, R. H.; Wang, S. D.; Wu, J.; Won, S. M.; Tao, H.; Islam, A.; *et al*. Epidermal Electronics. *Science* **2011**, *333*, 838–843.